LEVEL II

12

THE UNIVERSITY OF KANSAS CENTER FOR RESEARCH, INC.
2291 Irving Hill Drive—Campus West
Lawrence, Kansas 66045

(12)

ANALYTICAL STUDY OF THE BISTATIC RADAR CROSS-SECTION OF A PROLATE SPHEROID

Final Report

Prepared by

Albert W. Biggs
Principal Investigator

and

Stanton B. McMillian
Graduate Assistant

for

Office of Scientific Research
Bolling Air Force Base
Washington, D.C. 20332

Contract No. AFOSR-79-0105

March 1980

THE UNIVERSITY OF KANSAS CENTER FOR RESEARCH, INC.

2291 Irving Hill Drive—Campus West
Lawrence, Kansas 66045

LIST OF SYMBOLS

P_r	received signal power, watts
P_t	transmitter power, watts
G_t	transmitting antenna gain in the target direction
G_r	receiving antenna gain in the target direction
σ_b	bistatic radar cross-section, square meters
D_t	transmitter to target distance, meters
D_r	receiver to target distance, meters
$L_p(t)$	propagation loss over the transmitter to target path
$L_p(r)$	propagation loss over the receiver to target path
L_s	system loss
λ	wavelength, meters
U_r	power density at the receiver, watts per square meter
U_t	power density at the target, watts per square meter
$\vec{k}'$	unit vector in the direction of the reflected ray
$\vec{k}$	unit vector in the direction of the transmitted ray
t	distance from the target to the point of observation--may include or exclude the receiver
$\vec{N}$	unit vector normal to and outward from the prolate spheroidal surface
$P(x,y,z)$	point on the prolate spheroidal surface
$\vec{B}$	unit vector tangent to the circle formed by a plane intersecting the prolate spheroid normal to its axis.
$\vec{T}$	unit vector normal to $\vec{N}$ and $\vec{B}$

1.0 INTRODUCTION

Early experimental radar systems were predominantly of the bistatic type, where the transmitting and receiving antennas were usually separated by a distance comparable to the target distance [1] - [2]. When the duplexer was developed at the Naval Research Laboratory in 1936, a means of using the same antenna for transmitting and receiving made monostatic (one site) radar feasible. Bistatic radar became dormant until the early 1950's, when interest revived [1]. Interest has increased with the development of low level cruise missiles in 1978, when the need for bistatic cross-section results became apparent for missile guidance and target detection.

Bistatic radar systems utilize two separate locations. The radar transmitter is found at one location, while the radar receiver is found at another location. In some configurations, the radar transmitter might be located in a B-52 airplane and the radar receiver might be located in low altitude offensive air-to-ground missiles such as the AGM-69A. In other configurations, the radar transmitter would be located on the ground to control several ground-to-air defensive missiles. In the first example, the target could be an enemy missile silo or ground radar system. In the second example, it would be either the attacking offensive missiles or a B-52 guidance and control airplane. The parameters for detection include Doppler frequency shift from the target, signal frequency, and bistatic radar cross-section created by the target. This study is limited to the bistatic cross-section of a typical target. A prolate spheroid was selected because it resembles an air cruise missile. The air inlets and tail fins were not included in the analysis presented here. Results are presented in the form of bistatic cross-sections and

the computer program to generate additional cross-sections for prolate spheroids with different major to minor axis ratios.

2.0 BISTATIC RADAR CROSS-SECTIONS

The purpose of this study was to formulate the bistatic radar cross-section of a perfectly conducting prolate spheroid when the prolate spheroid is large compared to the wavelength of the incident radiation. There are many studies [3] - [7] on the monostatic backscatter from small prolate spheroids (prolate spheroids whose size is comparable to wavelength) and also with studies of field distributions at the boundary of the shadow where diffraction effects must be considered, but these are not considered here. Objects are almost always large compared to wavelength in detection applications, and detection is seldom done near the shadow region. In the region that we are concerned with, the geometrical theory of optics can be applied, and can be used to generate some insight into the bistatic cross-sectional area as a function of the spatial coordinates.

Theory:

The bistatic radar equation can be written in the following manner:

$$P_r = \frac{\sigma_b}{4\pi D_r^2 L_p(r)} \cdot \frac{1}{L_s} \cdot \frac{P_t G_t}{4\pi D_t^2 L_p(t)} \cdot \frac{G\lambda^2}{4\pi} \qquad (1)$$

where the symbols are defined in the prefix of this report. Eq. (1) is arranged to emphasize the motivating analysis in the derivation of the radar equation. The power density U_t reaching the target is

$$U_t = \frac{P_t G_t}{4\pi D_t^2 L_p(t)} , \qquad (2)$$

the effective capture area of the receiving antenna is

$$\frac{G_r \lambda^2}{4\pi} , \tag{3}$$

where $\lambda^2/4\pi$ is the universal antenna constant, and the power density U_r at the receiving site is

$$U_r = \frac{4\pi P_r L_s}{G_r \lambda^2} . \tag{4}$$

The system loss is assumed to occur only at the receiving system. Although it actually occurs in various locations, the exact location or even its existence do not effect the subsequent analysis. The use of Eqs. (2) and (4) can rewrite Eq. (1) as

$$U_r = \frac{\sigma_b}{4\pi D_r^2 L_p(r)} \quad U_t , \tag{5}$$

and the form of σ_b suitable for computation is

$$\sigma_b = 4\pi D_r^2 L_p(r) \frac{U_r}{U_t} , \tag{6}$$

and to numerical formulation if U_r can be found when U_t is given.

Figure 1 shows the case from geometrical optics of an incoming ray, $\vec{k}$, being reflected from a point on a curved surface in the direction, $\vec{k}'$. A very important point arises here with respect to the prolate spheroid. Since the object is convex, a one-to-one correspondence exists between reflection points and receiving points. As such, no interference exists between reflection points, and U_r can be described simply by $\vec{k}'$ and how energy density decreases as a function of distance between the reflection point and observation point. In other words,

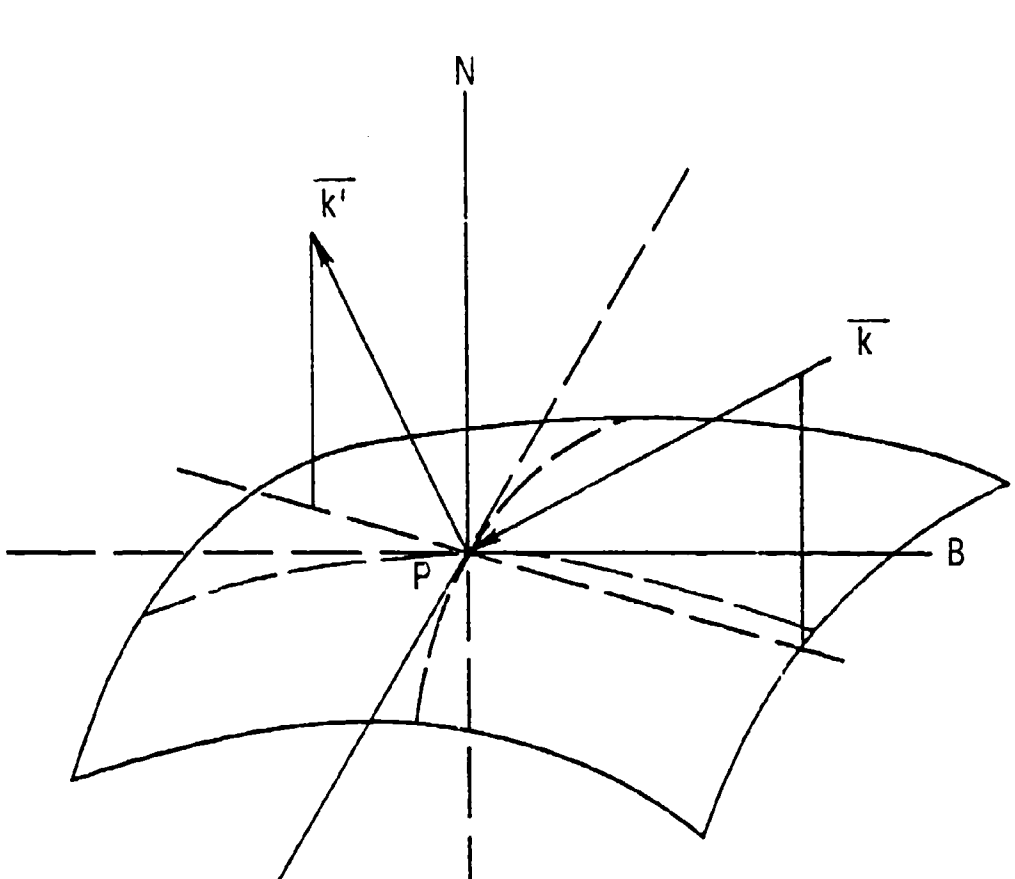

Figure 1

$$U_r = \frac{U_t}{\text{spread}(t\vec{k}')}, \tag{7}$$

where spread$(t\vec{k}')$ is a function describing the spreading out of energy as one travels in the $\vec{k}'$ direction.

Figure 1 also shows the coordinate system that is to be imposed at each point of the prolate spheroid. The prolate spheroid is described by the equation:

$$\frac{x^2+y^2}{\ell^2(u^2-1)} + \frac{z^2}{\ell^2 u^2} = 1, \tag{8}$$

which generates an outward normal unit vector at a point P = (x,y,z):

$$\vec{N} = C\left(x, y, z\,\frac{u^2-1}{u^2}\right) \tag{9}$$

where

$$C = \left(x^2+y^2+z^2\left(\frac{u^2-1}{u^2}\right)^2\right)^{-1/2} \tag{10}$$

It is convenient to define a coordinate system at P where $\vec{N}$ defines one axis, and

$$\vec{B} = \frac{(y,-x,0)}{\sqrt{x^2+y^2}} \tag{11}$$

and

$$\vec{T} = \vec{N} \times \vec{B} \tag{12}$$

define the other two. This choice of $\vec{B}$ is stimulated by the symmetry of the prolate spheroid. $\vec{B}$ is tangent to any circle defined by holding z constant and is normal to $\vec{N}$.

It is easily seen that the incident and reflected rays, $\vec{k}$ and $\vec{k}'$ respectively, lie in a plane containing $\vec{N}$ at P(x,y,z). Without loss of generality we can assume that both $\vec{k}$ and $\vec{k}'$ are unit vectors, and $\vec{k}'$ can be written

$$\vec{k}' = \vec{k} - 2\,(\vec{k}\cdot\vec{N})\vec{N}. \tag{13}$$

Having found the direction of the reflected energy, it is now necessary to derive an explicit expression for the spread function. Figure 2 demonstrates the underlying assumptions regarding the spread function. It is readily seen that all the power reflecting from the rectangle in the BT plane described by the sides $\lambda\vec{T}$ and $\gamma\vec{B}$ must pass through the surface described by the tips of the vectors $t\vec{k}_i'$. Define

$$\vec{R}_1 = \lambda\vec{T} + t\vec{k}_1' - t\vec{k}_0' \tag{14}$$

and

$$\vec{R}_2 = \lambda\vec{B} + t\vec{k}_2' - t\vec{k}_0' \tag{15}$$

These vectors describe the sides of the rectangle at the tips of the $t\vec{k}'_i$ and the spread function can now be defined:

$$\text{spread}(t\vec{k}_0') = \lim_{\substack{\lambda\to 0\\ \gamma\to 0}} \left| \frac{\vec{k}_0' \cdot \vec{R}_1 \times \vec{R}_2}{\vec{k}_0' \cdot \lambda\vec{T} \times \gamma\vec{B}} \right| . \tag{16}$$

Equation (16) is still not in a form that is amenable to implementation on a computer, but it can be made so very easily by approximating $\vec{k}'$, by the expression

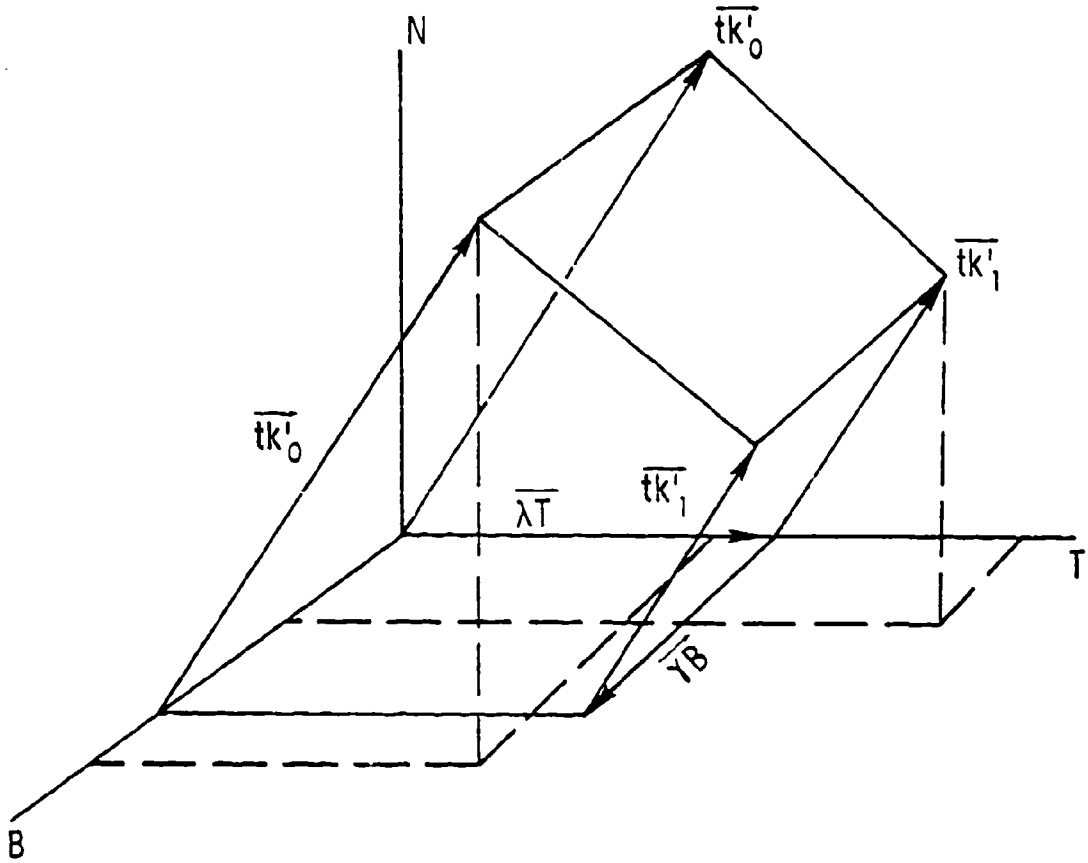
N
$\overline{tk'_0}$
$\overline{tk'_1}$
$\overline{tk'_0}$
$\overline{\lambda T}$
$\overline{tk'_1}$
T
$\overline{YB}$
B

Figure 2

$$\vec{k}_1' = \vec{k}_0' + \lambda \frac{d\vec{k}_o'}{d\lambda} , \tag{17}$$

where

$$\frac{d\vec{k}_o'}{d\lambda} = \left[\frac{d}{d\lambda} \vec{k}_o(x,y,z) + \lambda\vec{T}\right] \Bigg|_{\lambda \to 0} \tag{18}$$

and k'_1 similarly. Substituting Eq. (17) back into Eqs. (14) and (15) gives

$$\vec{R}_1 = \lambda(\vec{T} + t \frac{d\vec{k}_0'}{d\lambda}), \tag{19}$$

$$\vec{R}_2 = \gamma(\vec{B} + t \frac{d\vec{k}_0'}{d\lambda}), \tag{20}$$

and substituting these into Eq. (16) we finally arrive at:

$$\text{spread } (tk_0') = \left| \frac{\vec{k}_0' \cdot [-\vec{N} + t(\vec{T} \times \frac{d\vec{k}_0'}{d\gamma} + \frac{d\vec{k}_0'}{d\lambda} \cdot \times \vec{B}) + t^2(\frac{d\vec{k}_0'}{d\lambda} \times \frac{d\vec{k}_0'}{d\gamma})]}{\vec{k}_o' \cdot \vec{N}} \right| \tag{21}$$

The expressions involved in trying to evaluate $\frac{d\vec{k}_0'}{d\lambda}$ are cumbersome because it is necessary to know $\vec{k}'_0$ explicitly in terms of x, y, and z, but by examining Eq. (13) we can get

$$\frac{d\vec{k}_0'}{d\lambda} = -2(\vec{k}\cdot\frac{\partial\vec{N}}{\partial\lambda})\vec{N} - 2(\vec{k}\cdot\vec{N}) \frac{d\vec{N}}{d\lambda} , \tag{22}$$

and

$$\frac{d\vec{k}_0'}{d\gamma} = -2(\vec{k}\cdot\frac{\partial\vec{N}}{\partial\gamma})\vec{N} - 2(\vec{k}\cdot\vec{N}) \frac{d\vec{N}}{d\gamma} . \tag{23}$$

Equation (9) gives $\vec{N}$ in terms of x, y, and z, and $\frac{d\vec{N}}{d\lambda}$ and $\frac{d\vec{N}}{d\gamma}$ can be calculated and are given by the following:

$$\frac{d\vec{N}}{d\lambda} = C\left(T_x, T_y, T_z \frac{u^2-1}{u^2}\right) - C^2\left[xT_x + yT_y + zT_z\left(\frac{u^2-1}{u^2}\right)^2\right], \tag{24}$$

$$\frac{d\vec{N}}{d\gamma} = C\left(B_x, B_y, B_z \frac{u^2-1}{u^2}\right) - C^2\left[xT_x + yT_y + zT_z\left(\frac{u^2-1}{u^2}\right)^2\right]\vec{N}. \tag{25}$$

Finally, referring to Eq. (6)

$$\sigma_b = 4 D_r^2 L_p(r) \frac{U_r}{U_t}, \tag{26}$$

assuming that $D_r = t$ and that $L_p(r) = 1$, we get

$$\sigma_b = \frac{4\pi t^2}{\text{spread}(t\vec{k}_0')} \tag{27}$$

It will be noticed that Eq. (21) for the spread function involves terms in 1, t and t^2. σ_b is usually examined in the limit as $t \to \infty$. σ_b then becomes

$$\sigma_b = \frac{4\pi|\vec{k}_0' \cdot \vec{N}|}{\left|\vec{k}_0' \cdot \frac{d\vec{k}_0'}{d\lambda} \times \frac{d\vec{k}_0}{d\gamma}\right|}. \tag{28}$$

3.0 RESULTS

Appendix 1 is a listing of the program that was used to find the bistatic cross-sectional area. SB is the cross-sectional area as given by Eq. (28) while SIGMAB is the value given by Eq. (22), retaining the t^{-1} and t^{-2} terms in the final expression.

Appendix 2 is a graphical representation of some of the results of this program.

Figure 3 shows the coordinate system used to orient the prolate spheroid in space. The major axis of the prolate is the z axis. The transmitter is located in the y, z plane which, because of the symmetry involved, does not affect the generality of the program.

Graphs 1-4 show σ_b for various transmitter positions. The observation plane is the y,z plane. The prolate spheroid has major axis one unit long, and minor axis .33 units long. σ_b is in square units.

Graph 5 shows σ_b for a sphere of a radius one unit.

Graphs 6, 7, 8 show σ_b in varying cases when the observation plane is not the y,z plane. (These are all for a prolate spheroid with major to minor axis ratio of 3:1). The observation plane in Graph 6 contains the z axis, but is at 45° with respect to the y axis. In Graph 7, the observation plane is the x,z plane. In Graph 8, the observation plane is the x, z plane, but rather than having the transmitter on the y axis as in Graphs 7 and 8, the transmitter is at 30° with respect to the z axis in the y,z plane.

Graph 9 shows σ_b when the major axis to minor axis ratio is changed from 3:1 to 10:1. In all other respects, this is the same as Graph 2.

The observation distance was equal to 1000 units in all the graphs.

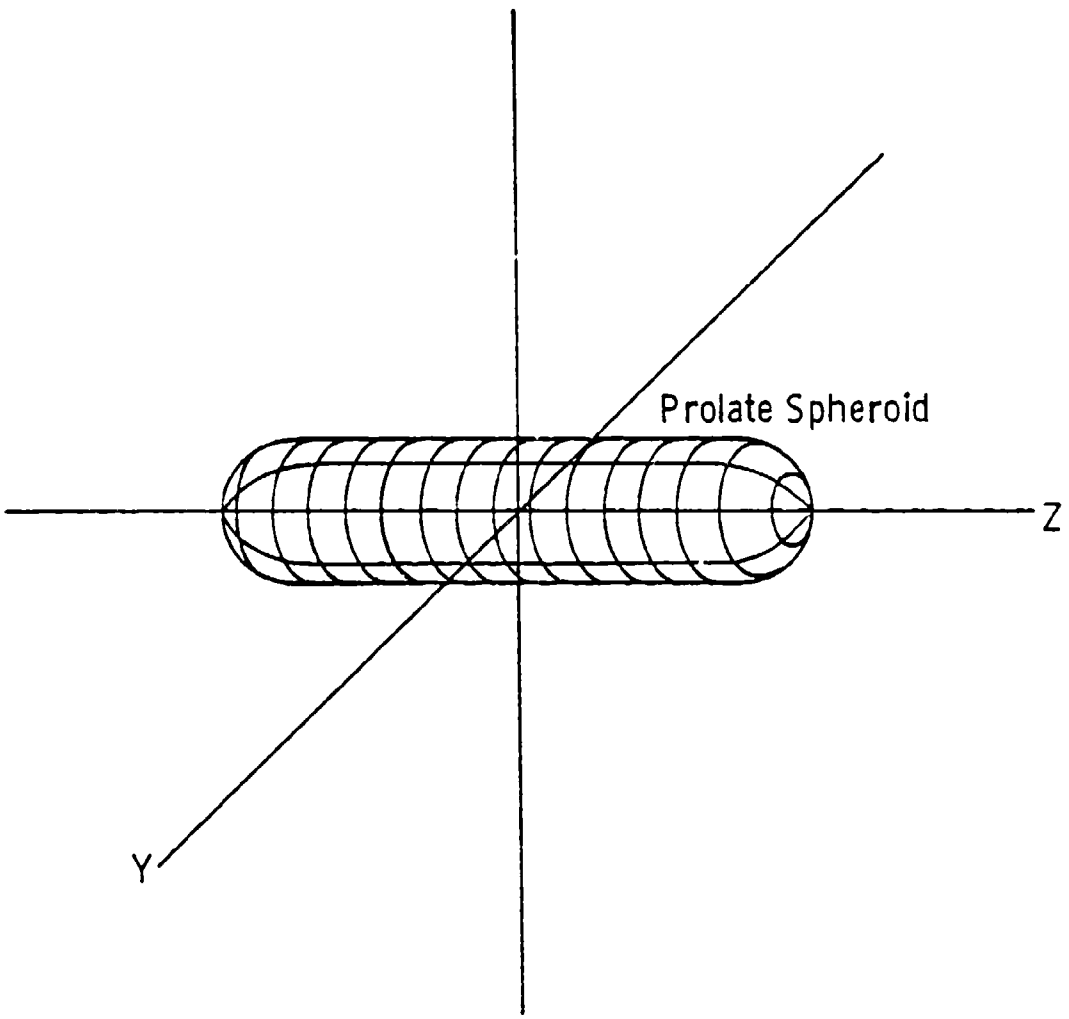

Figure 3

It will be seen immediately that for a prolate spheroid with major axis, 1 unit, the maximum value of σ_b is π. Graphs 1-4 show that this maximum value in the y-z plane is at 180° minus the transmitter angle which is exactly as expected in terms of reflections, and geometrical optics. It is also interesting to note that the patterns in Graphs 1-4 are exactly the same except for being rotated in space.

Graphs 4, 6, and 7 show another aspect of this pattern in space. The pattern has maximum width in the plane containing the transmitter and z axis, and becomes increasingly narrow as we rotate the observation plane away from the y,z plane. It is to be noted that the value of σ_b as we approach the shadow becomes undeterminate. In the x,y plane, $\sigma_b = \pi$ for all angles, while in the y,z plane, σ_b approaches .02702.

Graphs 2 and 8 show the same behavior as Graphs 4,6 and 7, except that the transmitter is now at an angle of 30° with respect to the z axis rather than being on the y axis. Again, the pattern approaches being infinitely thin, and is indeterminate as we approach the shadow.

Lastly, a comparison of Graphs 2 and 9 shows the effect of increasing the major axis to minor axis ratio. If the prolate spheroid becomes narrower the maximum value remains π, but the pattern becomes much narrower.

4.0 EVALUATION

The first question that must be asked is whether the results obtained have any meaning. First, the monostatic cross-sectional area, σ_m, for a prolate spheroid with the transmitter on the z axis is a well-known quantity [6] and

$$\sigma_m = \frac{\pi(u^3-1)^2 \ell^2}{u^2} \tag{29}$$

For a sphere, $\sigma_m = \pi$, which is within .1% of the value found using the program. For a prolate spheroid with major axis to minor axis ratio 3:1, ($u = 1.05$, $\ell = .95$), the program gives $\sigma_b = .02702$, while Eq. (29) gives $\sigma_m = .02702$. In fact, for ratios 3:1, 10:1, and 22:1, the agreement was exact.

Second, the Crispin bistatic theorem [8] stipulates that given transmitter and receiver directions, $\vec{k}$ and $\vec{k}'$ respectively, in the limit of infinite distance, σ_b is equal to σ_m as seen from the $\vec{k}$ and $\vec{k}'$ direction. Table 1 gives σ_b and σ_m for various transmitter and receiver locations. (The angles listed are with respect to the z axis).

As can be seen from Table 1, there is close agreement between σ_b and σ_m. The small discrepancies shown in the last two entries are easily accounted for when we consider that since the distance is not infinite, we are not looking at the same point on the prolate spheroid when calculating σ_b and σ_m.

We can conclude, then, that the program is giving meaningful numbers, and that these numbers do represent the bistatic cross-sectional area of a prolate spheroid.

5.0 CONCLUSION

The prolate spheroid is a convenient target for radar studies because it is convex. From a geometrical optics point of view, this is convenient because it implies that given an observation point, there is only one point on the prolate spheroid at which reflection occurs. As such, there is no need to account for the phase of the signal. Any surface that

is convex at each point, and which has no two distinct points where the outward normal vectors are in the same direction, can be handled similarly. Hence, the program written could very quickly be changed to handle a figure that is ellipsoidal in all the major planes, or even a parabola of revolution that extends to infinity in one direction. It is simply a matter of being able mathematically to describe the surface.

When the outward normal vectors are not distinct, it is necessary to account for the e^{ikr} spatial variations in both the incident and reflected fields. This can be done, but was beyond the scope of this study in both computer funds and time available.

Such a program would be a major step forward in the ability to find the bistatic cross-sectional area of arbitrary surfaces in space, where it is not clear that the Crispin Bistatic Theorem is appropriate. This would be an area for further study.

TABLE 1

A COMPARISON OF σ_b AND σ_m FOR THE CRISPIN BISTATIC THEOREM

Transmitter Location (degrees)	Receiver Location (degrees)	σ_b (units) (squared)	σ_m at $\vec{k} + \vec{k}'$
30°	-30°	.02702	.02702
60°	-60°	.02702	.02702
30°	150°	3.126	3.126
0°	60°	.04522	.04520
30°	90°	.26481	.26464

(The observation point is 1000 units away).

REFERENCES

[1] Skolnik, M.I., Introduction to Radar Systems, Chapter 36, McGraw-Hill, New York, 1962.

[2] Williams, A.F., The Study of Radar, pp. 434-440, Butterworth Scientific Publications, London, 1953.

[3] Buchholz, H., Die Konfluente Hypergeometrische Funktion, Springer-Verlag, Berlin, 1953.

[4] Kazarinoff, N.D. and Ritt, R.K., "On the theory of scalar diffraction and its application to the prolate spheroid," Ann. Physics, Vol. 6, pp. 277-299, 1959.

[5] Olte, A. and Silver, S., "New results in backscattering from cones and spheroids," IRE Trans. Ant. and Prop., Vol. AP-7, pp. 561-567, 1959.

[6] Siegel, K.M., Schultz, F.V., Gere, B.H., and Sleator, F.B., "The theoretical and numerical determination of the radar cross-section of a prolate spheroid," IRE Trans. Ant. and Prop., Vol. AP-4, pp. 266-275, 1956.

[7] Goodrich, R.F. and Kazarinoff, N.D., "Scalar diffraction by prolate spheroids whose eccentricities are almost one," Proc. Cambr. Phil. Soc., Vol. 59, pp. 167-183, 1962.

[8] Crispin, J.W., Jr., et al., "A theoretical method for the calculation of radar cross-sections of aircraft and missiles," University of Michigan Radiation Lab. Report 2591-1-H, July 1959.

APPENDIX A

```
C THIS PROGRAM CALCULATES THE BISTATIC CROSS SECTIONAL AREA OF A
C PROLATE SPHEROID.  L AND U ARE PARAMETERS THAT DESCRIBE THE
C SPHEROID.  U CAN NEVER BE LESS THAN ONE.
      REAL L,U,THETA,K,P(3),W1,ESTKP(3)
      REAL K(3),B(3),N(3),T(3),KPRIME(3),DLN(3)
      REAL DGN(3),DLKP(3),C1(3),C2(3),DGKP(3)
      REAL FL(3),FG(3),SB,DIST,SIGMAB,OBSPNT(3)
      INTEGER I,J,M,JP,INCAY,INCAZ
      LOGICAL TEST, RETEST
      REAL MAG,ALPHA,BETA,KDIST

      PRINT, ' L = '
      READ(5,200) L
200   FORMAT(F10.5)
      PRINT, ' U = '
      READ(5,200) U
      PRINT, 'THETA = '
      READ(5,200) THETA
      WRITE(03,104) L,U,THETA
104   FORMAT(' L = ',F8.4,' U = ',F8.4,' THETA = ',F8.0)

C K IS THE VECTOR THAT DESRIBES THE DIRECTION OF THE INCOMING
C RADIATION.  THE ANGLE THETA IS BETWEEN 0 AND 90, INCLUSIVE.
      PI = ARCOS(-1.0)
      THETA = PI*THETA/180.0
      K(1)=0
      K(2) = -1.0*SIN(THETA)
      K(3) = -1.0*COS(THETA)

      PRINT,' DISTANCE = '
      READ(5,201) DIST
201   FORMAT(' ',F10.1)
      PRINT, ' INCR OF ANGLE IN Y = (I3) '
      READ(5,202) INCAY
      PRINT, ' INCR OF ANGLE IN Z = (I3) '
      READ(5,202) INCAZ
202   FORMAT(I3)
      RETEST=.FALSE.
      DO 10 J=1,181,INCAY
      BETA= J-1
      BETA= PI*BETA/180.0
      DO 20 M=1,181,INCAZ
      IF(RETEST.AND.M.EQ.1) GO TO 20
      IF(M.EQ.1) RETEST = .TRUE.
      ALPHA = M-1
      ALPHA = PI*ALPHA/180.0
C CONVRT TAKES THE DISTANCE AND ANGLES, AND CONVERTS THESE TO THE
C POINT DESIRED.
      CALL CONVRT(DIST,ALPHA,BETA,OBSPNT)
      WRITE(03,105) OBSPNT
105   FORMAT(' THE OBSERVATION POINT = ',3(F8.0,4X))
```

```
      TEST = .FALSE.
C IF THE POINT IS TOO CLOSE TO THE AXIS THAT K IS ON,
C THEN THE ROUTINES BLOW UP.
      IF((MAG(OBSPNT)-DOT(OBSPNT,K)).LE.1.0E-10) TEST = .TRUE.
      IF(TEST) GO TO 40
      C=OBSPNT(1)**2+OBSPNT(2)**2+(U**2-1.0)*(OBSPNT(3)/U)**2
      IF(C.LE.L**2) TEST=.TRUE.
      IF(TEST) WRITE(03,107) ' OBSPNT TOO SMALL '
107   FORMAT(' ',A20)
      IF(TEST) GO TO 20

C THE PROGRAM NOW GOES ABOUT IMPOSING AN N,B,T FRAME ON THE
C SPHEROID AT THE POINT OF REFLECTION.  INCIDENTALLY, IT MUST FIRST
C FIND THE POINT OF REFLECTION.  HENCE, FINDKP.
      CALL NORM(OBSPNT,C1)
      CALL SUB(C1,K,C1)
      CALL NORM(C1,N)

106   C=L*(U**2-1.0)/SQRT((U**2-1.0)*(N(1)**2+N(2)**2)+U**2*N(3)**2)
      P(1)=C*N(1)
      P(2)=C*N(2)
      P(3)=C*U**2/(U**2-1.0)*N(3)
      CALL FINDKP(P,N,B,T,KPRIME)
      CALL SUB(OBSPNT,P,ESTKP)
      CALL NORM(ESTKP,ESTKP)
      CALL ADD(KPRIME,ESTKP,C1)
      CALL NORM(C1,KPRIME)
      CALL SUB(KPRIME,K,C1)
      CALL NORM(C1,N)
      CALL SUB(KPRIME,ESTKP,ESTKP)
      IF(MAG(ESTKP).GT.1.0E-4) GO TO 106

      IF(DOT(P,K).GE.0.0) TEST = .TRUE.
40    IF(TEST) WRITE(03,107) ' IN THE SHADOW '
      IF(TEST) GO TO 20
      CALL SUB(OBSPNT,P,C1)
      KDIST = MAG(C1)


C IT IS NECESSARY TO DETERMINE FEATURES OF THE CURVATURE OF THE
C SPHEROID AT THE POINT OF REFLECTION.  THE DERIVATIVES OF N ARE
C TAKEN IN THE N AND T DIRECTIONS.  LAMBDA, AND GAMMA ARE
C DUMMY COORDINATE DESCRIPTIONS IN THE TWO DIRECTIONS.
      CALL DERIV(P,N,B,DLN)
      CALL DERIV(P,T,B,DGN)
      IF(DOT(DLN,B).GT.0.0) CALL SCALT(-1.0,DLN,DLN)
      IF(DOT(DGN,B).GT.0.0) CALL SCALT(-1.0,DGN,DGN)
```

```
C USING DLN AND DGK, IT IS POSSIBLE TO CALCULATE THE DERIVATIVE OF
C KPRIME, THE VECTOR FROM THE POINT ON THE P.S. TO THE OBSERVATION
C POINT, IN THE TWO DIRECTIONS, AND THEN TO FIND THE SPREAD OF THE
C RADIATION AS IT TRAVELS AWAY FROM THE P.S.
      CALL SCLMLT(DOT(N,K),DLN,C1)
      CALL SCLMLT(DOT(DLN,K),N,C2)
      CALL ADD(C1,C2,DLKP)
      CALL SCLMLT(-2.0,DLKP,DLKP)
      CALL SCLMLT(DOT(N,K),DGN,C1)
      CALL SCLMLT(DOT(DGN,K),N,C2)
      CALL ADD(C1,C2,DGKP)
      CALL ADD(C1,C2,DGKP)
      CALL SCLMLT(-2.0,DGKP,DGKP)
      CALL CROSS(U,DGKP,C1)
      CALL CROSS(DLKP,T,C2)
      CALL ADD(C1,C2,C1)
      CALL SCLMLT(1.0/KDIST,C1,C1)
      CALL SCLMLT(1.0/KDIST**2,U,C2)
      CALL ADD(C1,C2,C1)
      CALL CROSS(DLKP,DGKP,C2)
C SB IS THE BISTATIC CROSSSECTIONAL AREA IF WE IGNORE THE D AND
C D**2 TERMS IN THE SPREAD EXPRESSION.
      SB=4.0*PI*DOT(N,KPRIME)/DOT(C2,KPRIME)
      IF(SB.LT.0.0) SB=-1.0*SB
      CALL ADD(C1,C2,C2)
C SIGMAB IS THE TRUE CROSSSECTIONAL AREA.
      SIGMAB=4.0*PI*DOT(N,KPRIME)/DOT(C2,KPRIME)
      IF(SIGMAB.LT.0.0) SIGMAB=-1.0*SIGMAB
      WRITE (03,102) 'SB = ',SB,'  SIGMAB = ',SIGMAB
102   FORMAT(' ',A5,F10.5,A11,F10.5)
20    CONTINUE
10    CONTINUE
      STOP
      END
      REAL FUNCTION MAG(A)
      REAL A(3)
      MAG=SQRT(A(1)**2+A(2)**2+A(3)**2)
      RETURN
      END
      SUBROUTINE UNIV(A,B)
      REAL A(3),B(3), C, MAG
      C=SQRT(A(1)**2+A(2)**2+A(3)**2)
      IF(C.LE.1.0E-20)  WRITE(03,12) ' DIVISION BY ZERO '
12    FORMAT(' ',A14)
      C=1.0/C
      CALL SCLMLT(C,A,B)
      RETURN
      END
```

```
      SUBROUTINE FINDKP(K,N,H,T,KPRIME)
      REAL K(3),N(3),B(3),T(3),KPRIME(3)
      REAL C1(3),C2(3),MAG
      B(1)=(N(2))
      B(2)=-N(1)
      B(3)=0.0
      IF(MAG(B).LE.1.0E-20) B(1)=1.0
      CALL NORM(B,B)
      CALL CROSS(N,B,T)
      CALL SCLMLT(-2.0*DOT(K,T),N,C1)
      CALL ADD(K,C1,KPRIME)
      RETURN
      END

      SUBROUTINE ADD(A,B,C)
      REAL A(3), B(3), C(3)
      INTEGER I
      DO 10 I=1,3
      C(I)=A(I)+B(I)
10    CONTINUE
      RETURN
      END
      SUBROUTINE SUB(A,B,C)
      REAL A(3),B(3),C(3)
      INTEGER I
      DO 10 I=1,3
      C(I)=A(I)-B(I)
10    CONTINUE
      RETURN
      END

      SUBROUTINE SCLMLT(A,B,C)
      REAL A,B(3),C(3)
      INTEGER I
      DO 10 I=1,3
      C(I)=A*B(I)
10    CONTINUE
      RETURN
      END

      REAL FUNCTION DOT(A,B)
      REAL A(3),B(3)
      INTEGER I
      DOT=0
      DO 10 I=1,3
      DOT = DOT+A(I)*B(I)
10    CONTINUE
      RETURN
      END
```

```
      SUBROUTINE CROSS(A,B,C)
      REAL A(3),B(3), C(3)
      C(1)=A(2)*B(3)-A(3)*B(2)
      C(2)=A(3)*B(1)-A(1)*B(3)
      C(3)=A(1)*B(2)-A(2)*B(1)
      RETURN
      END

      SUBROUTINE CONVRT(A,B,C,D)
      REAL A,B,C,D(3)
      REAL P,Q
      LOGICAL TEST
      TEST = .FALSE.
      D(1)=0.0
      D(2) = A*SIN(B)
      D(3) = A*COS(B)
      IF(SIN(C)**2.LT.1.0E-10.AND.COS(C).GT.0.0)RETURN
      IF(SIN(C)**2.LT.1.0E-10) TEST = .TRUE.
      IF(TEST) D(2)=-A*SIN(B)
      IF(TEST) D(3)=-A*COS(B)
      IF(TEST) RETURN
      IF(SIN(B)**2.LT.1.0E-10) RETURN
      IF(COS(B)**2.LT.1.0E-10) P = 0.0
      IF(COS(C)**2.LT.1.0E-10) Q = 0.0
      IF(COS(B)**2.GT.1.0E-10) P = 1.0/TAN(B)
      IF(COS(C)**2.GT.1.0E-10) Q = 1.0/TAN(C)
      D(1)=A/SQRT(1.0+(Q)**2+(P)**2)
      D(2)=D(1)*Q
      D(3)=D(1)*P
      RETURN
      END
      SUBROUTINE DERIV(P,T,U,DLD)
      REAL P(3),T(3),U,DLD(3)
      REAL A(3),B(3),C(3),D(3),MAG
      A(1)=P(1)
      A(2)=P(2)
      A(3)=P(3)*(U**2-1.0)/U**2
      B(1)=T(1)
      B(2)=T(2)
      B(3)=T(3)*(U**2-1.0)/U**2
      CALL SCLMLT(1.0/MAG(A),B,C)
      CALL SCLMLT(DOT(A,B),A,D)
      CALL SCLMLT(1.0/MAG(A)**3,D,D)
      CALL SUB(C,D,DLD)
      RETURN
      END
```

APPENDIX B

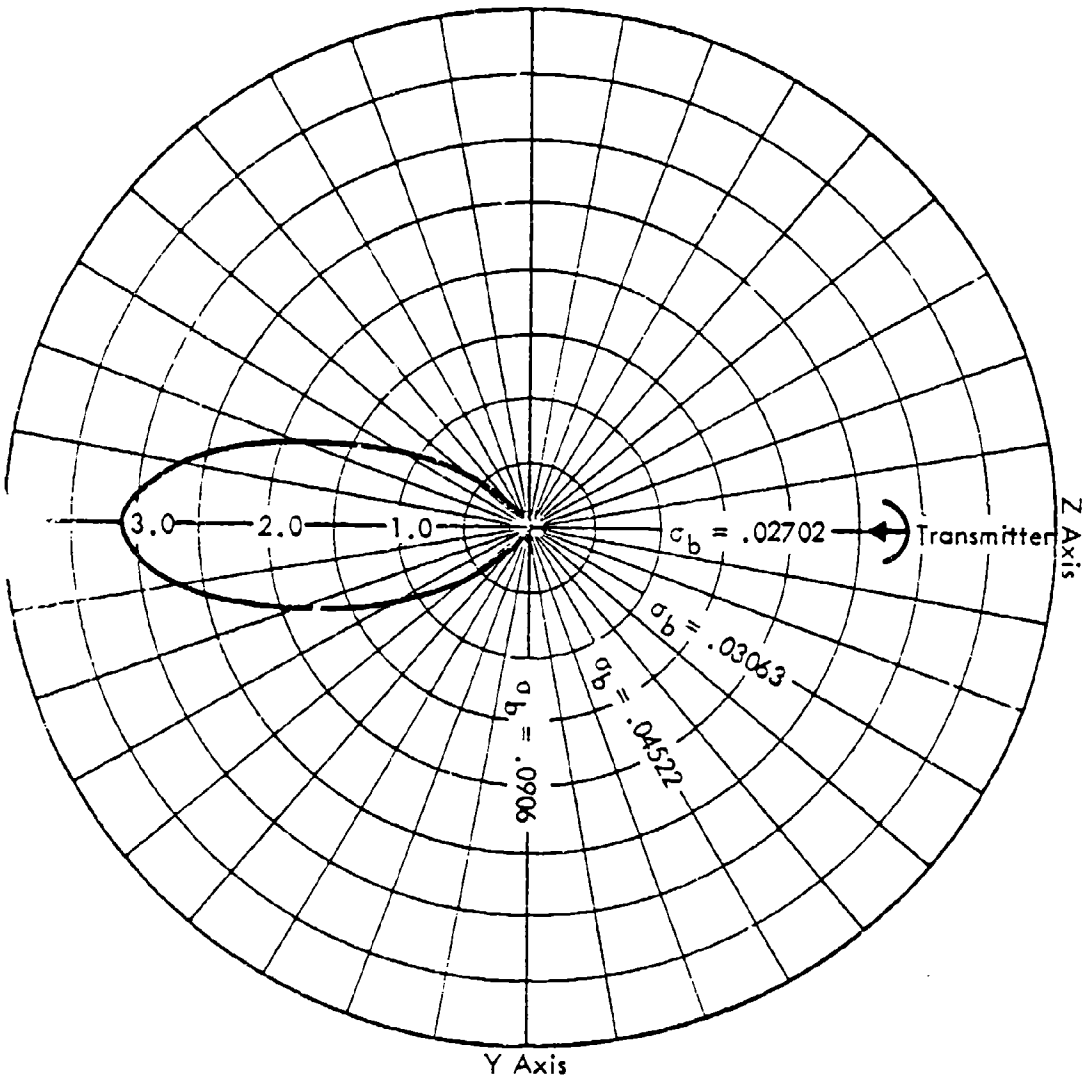

Graph 1: Bistatic Radar Cross-Sectional Area of a Prolate Spheroid (major to minor axis ratio 3:1)

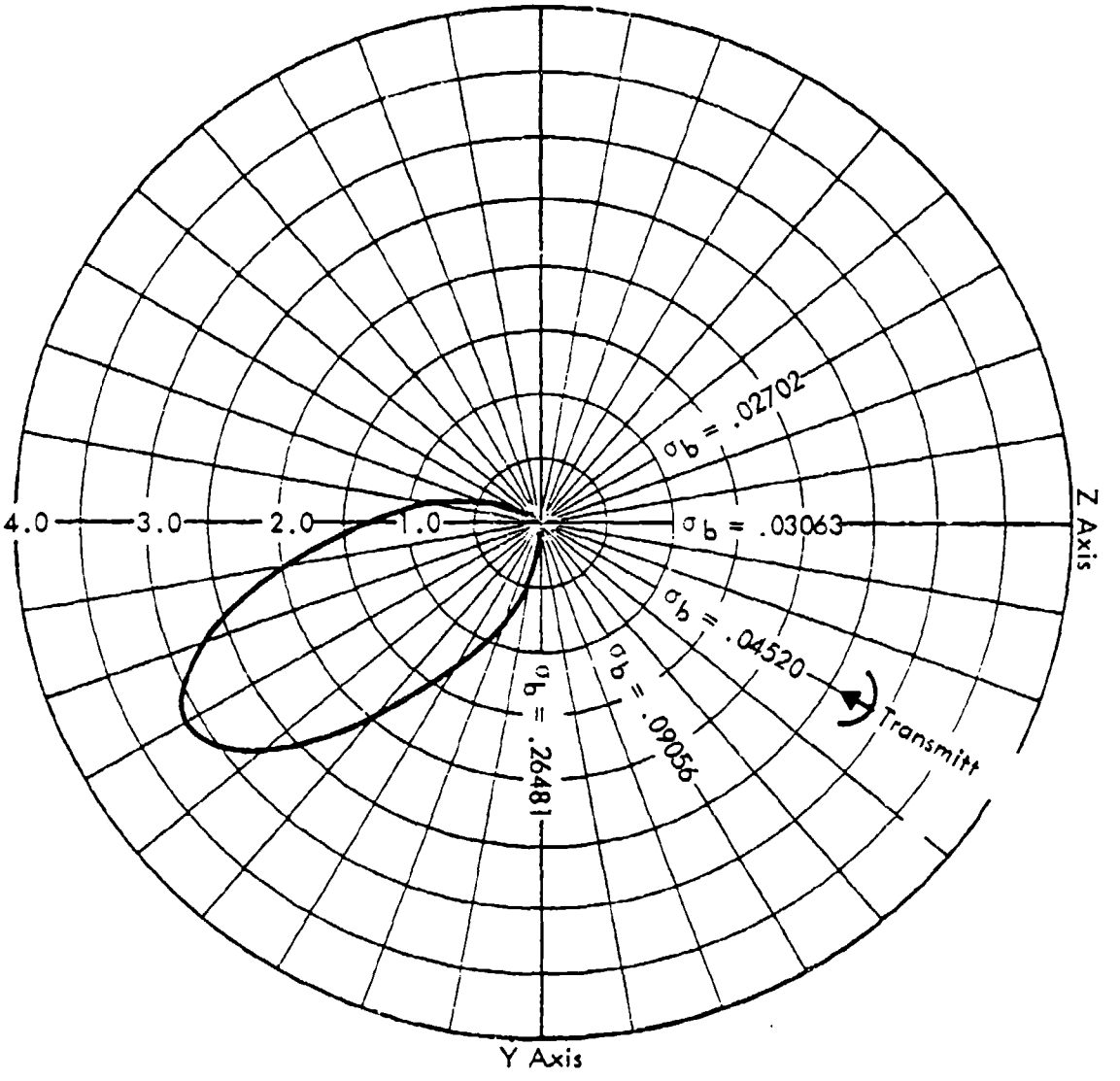

Graph 2: σ_b for a Prolate Spheroid with the Transmitter at 30° w.r.t. the Z Axis (major to minor axis ratio 3:1)

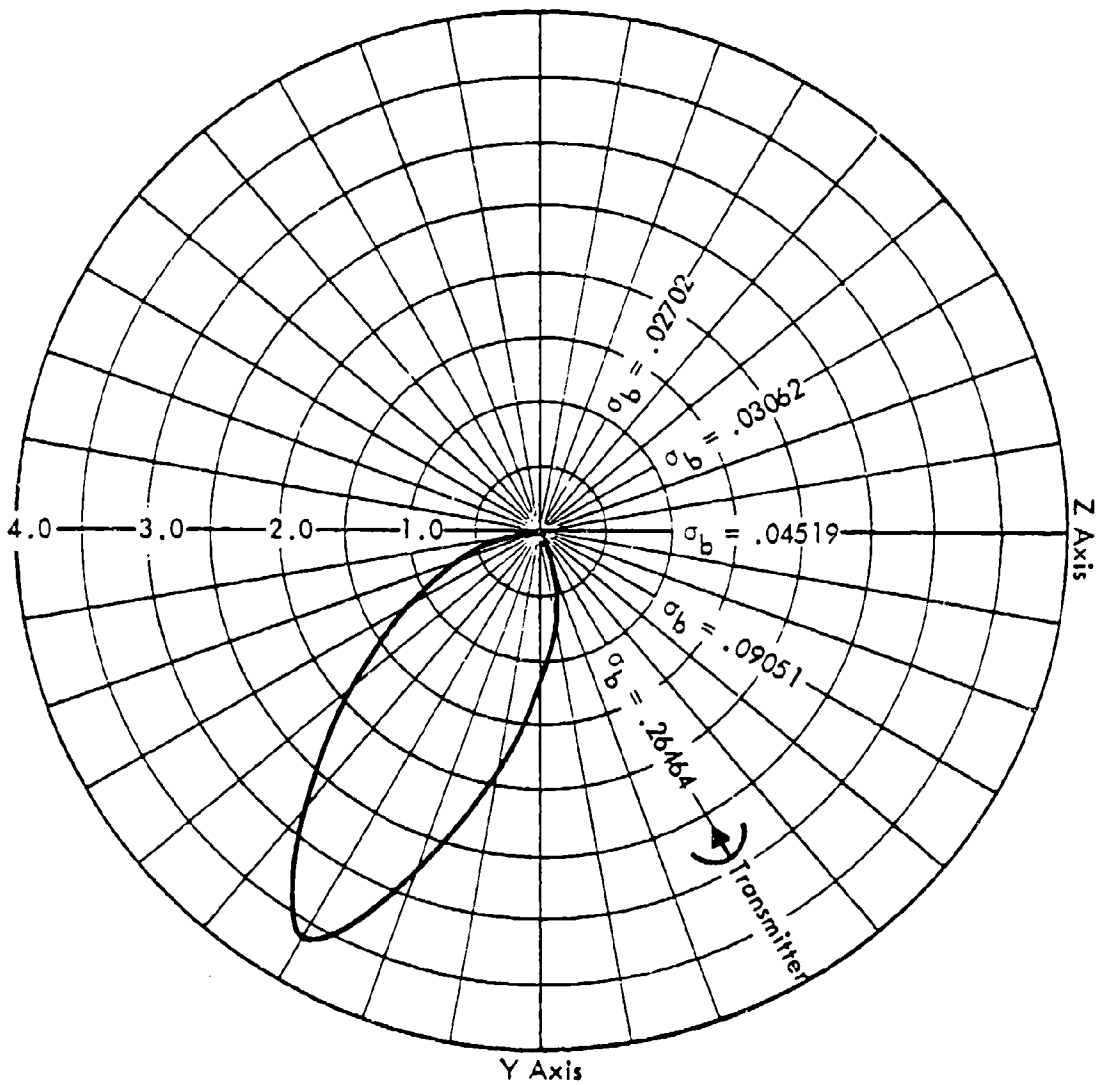

Graph 3: σ_b for a Prolate Spheroid with the Transmitter at 60° w.r.t. the Z Axis (major to minor axis ratio 3:1)

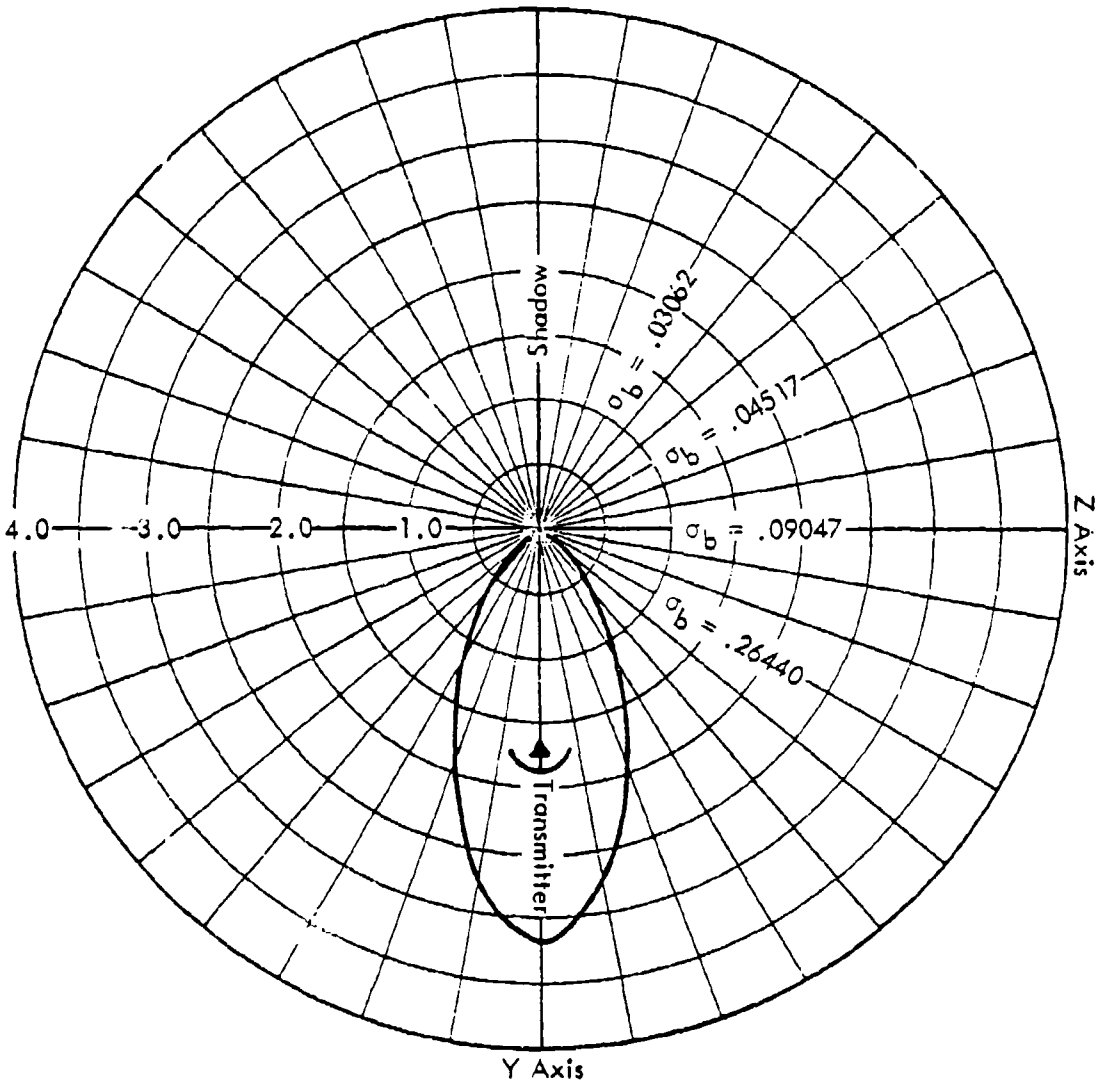

Graph 4: σ_b for a Prolate Spheroid with the Transmitter at 90° w.r.t. the Z Axis (major to minor axis ratio 3:1)

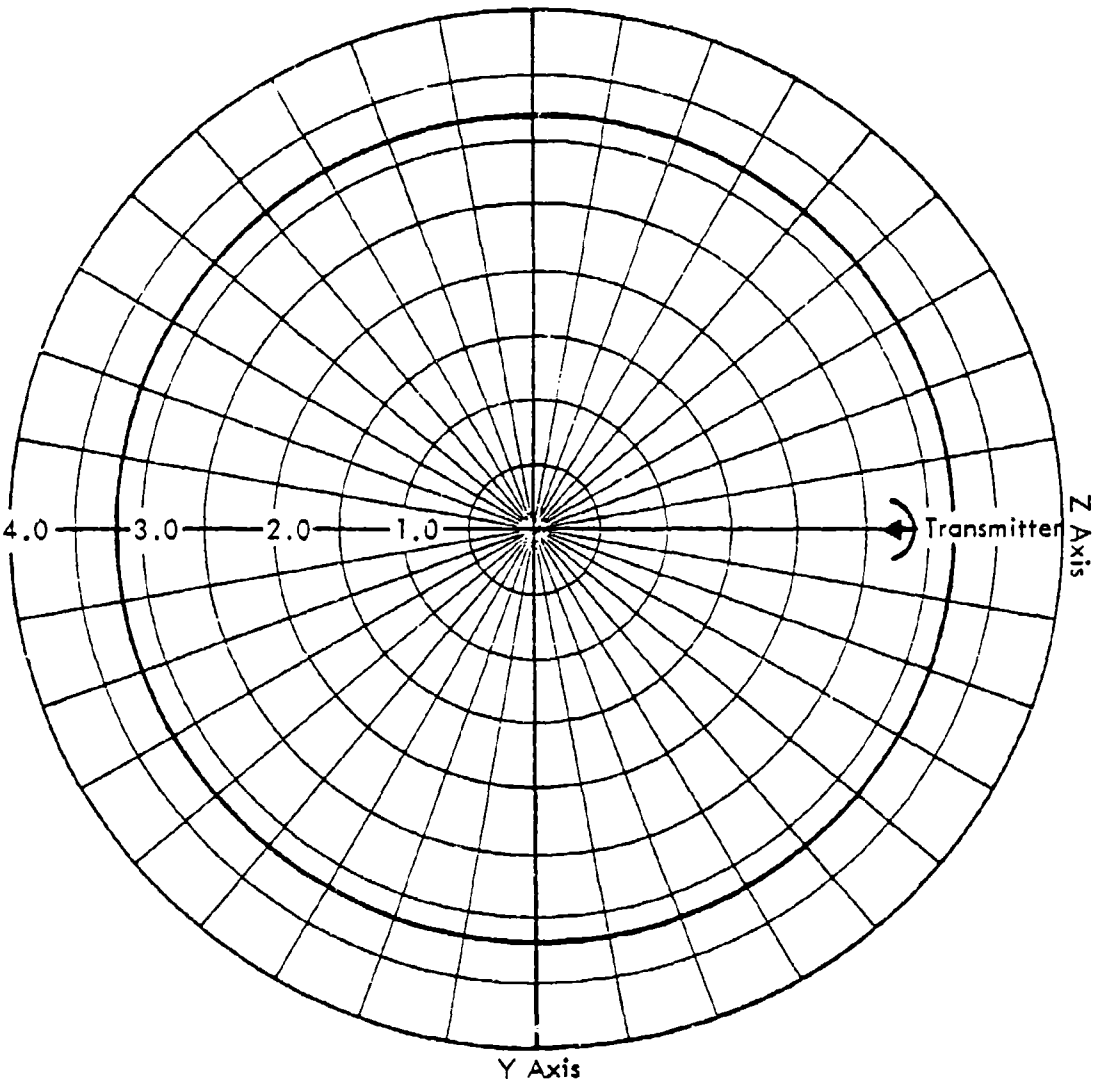

Graph 5: σ_b for a Sphere of Radius 1 Unit

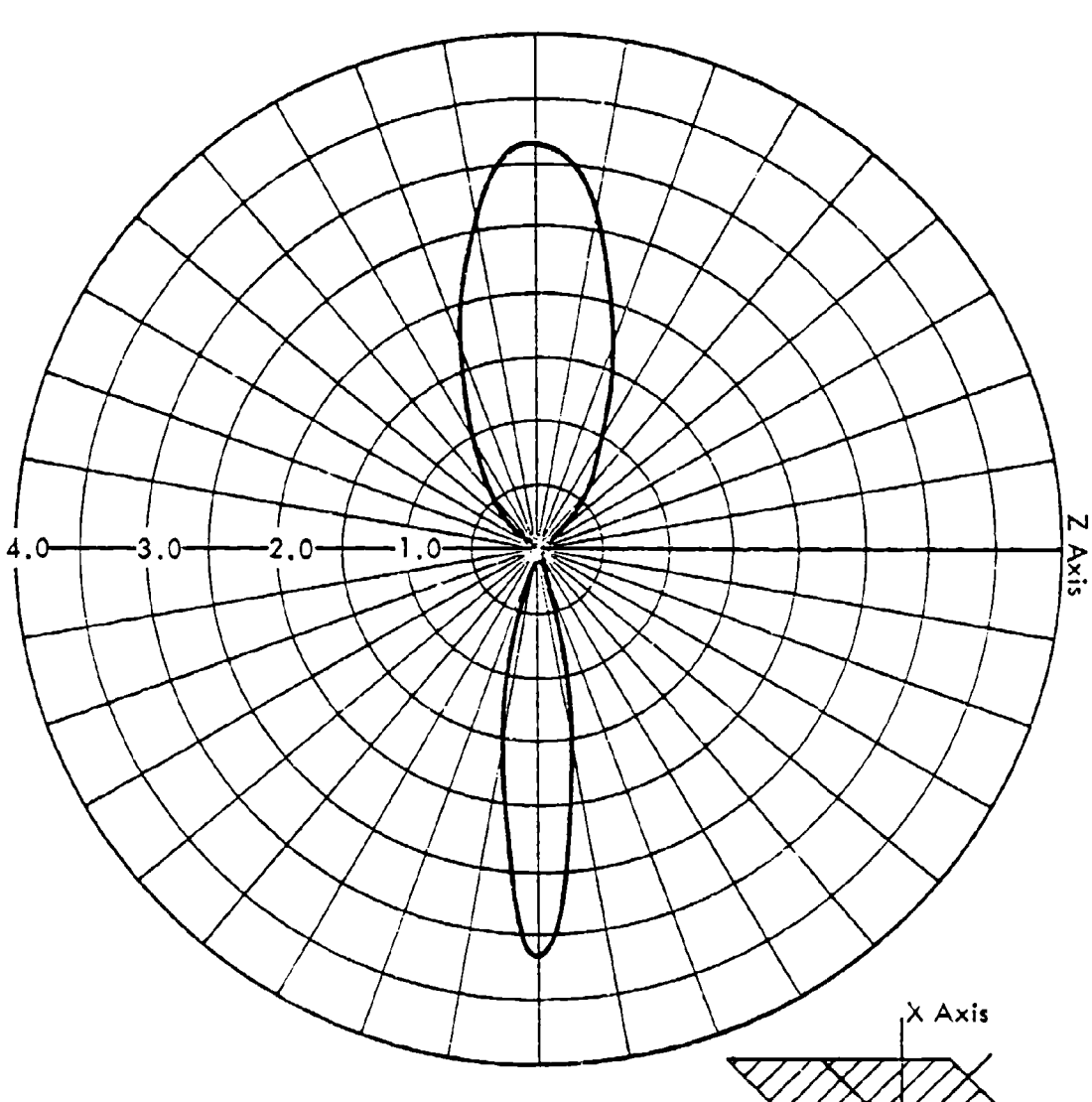

Graph 6: σ_b for a Prolate Spheroid with the Observation Plane at 45°
(major to minor axis ratio 3:1)

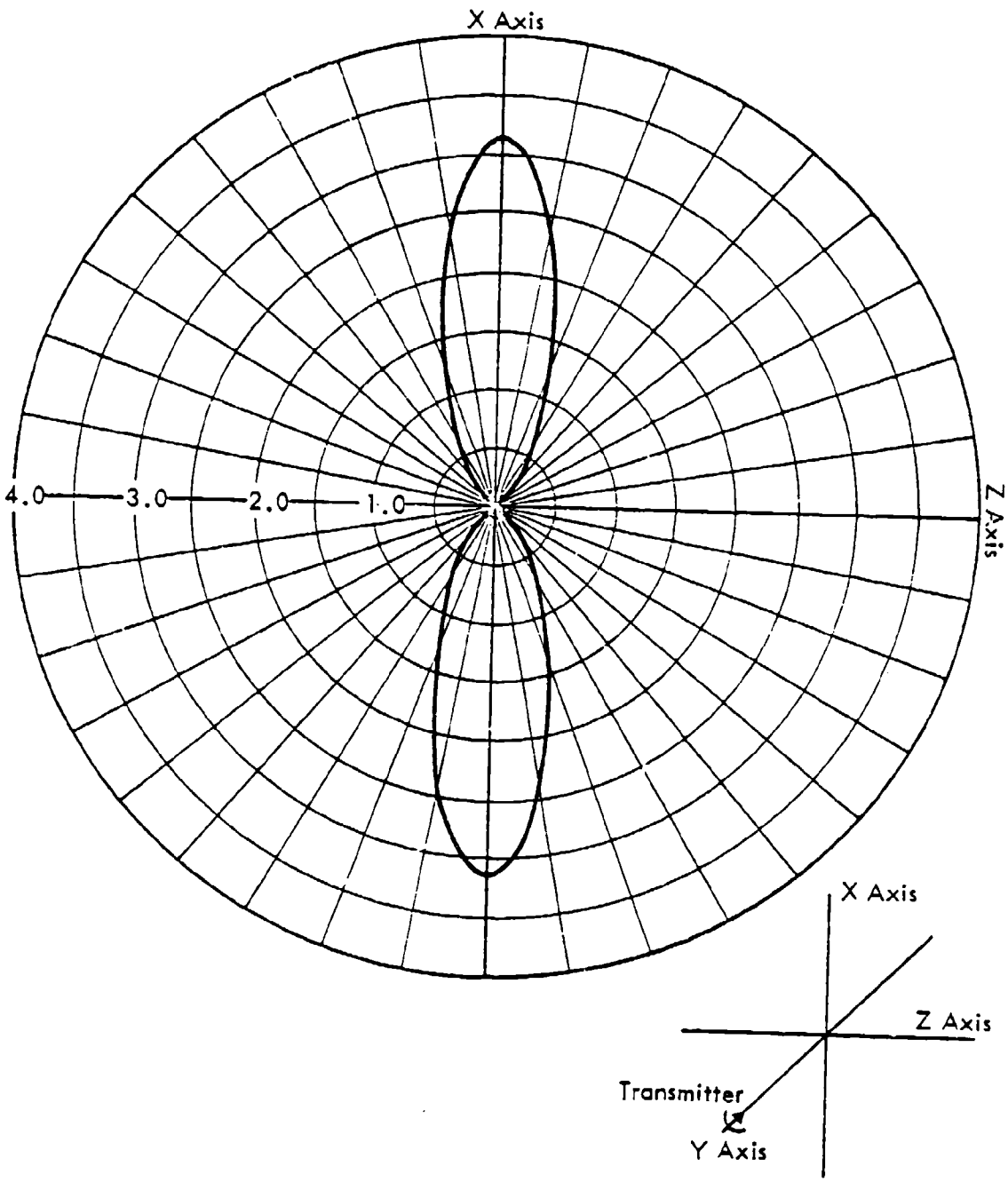

Graph 7: σ_b for a Prolate Spheroid with the Observation Plane Being the X, Z Plane (major to minor axis ratio 3:1)

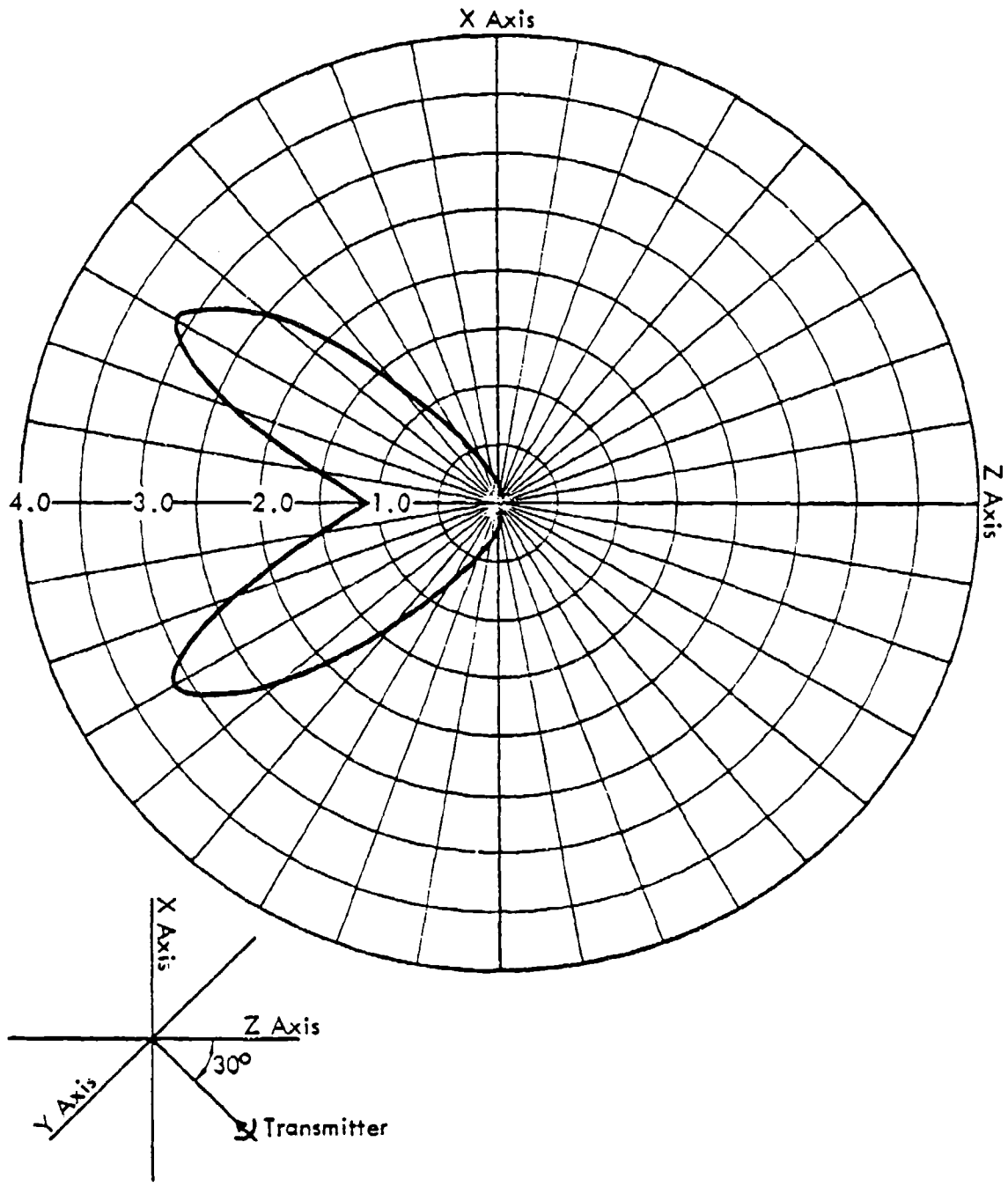

Graph 8: σ_b for a Prolate Spheroid with the Transmitter at 30° w.r.t. the Z Axis, with the Observation Plane being the X, Z Plane (major to minor axis ratio 3:1)

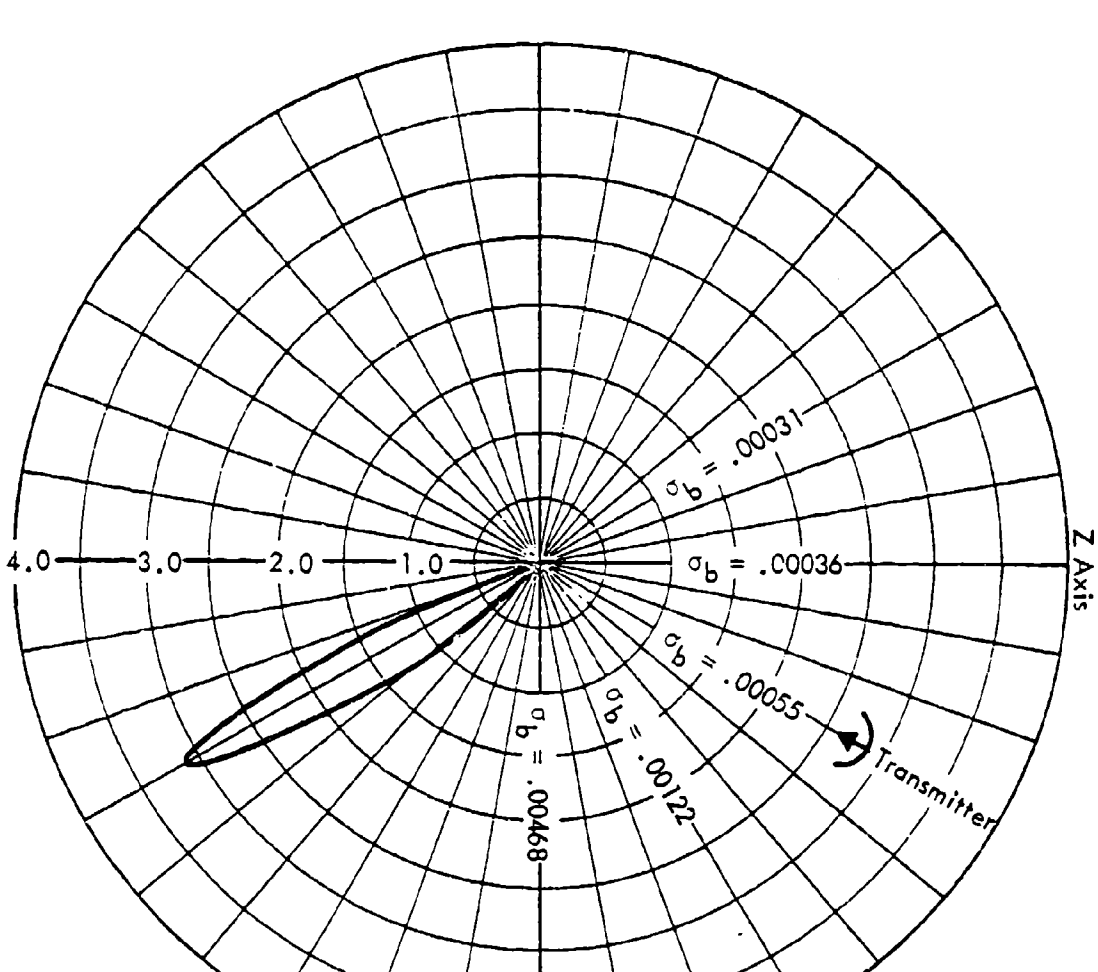

Graph 9: σ_b for a Prolate Spheroid with Major to Minor Axis Ratio 10:1 with the Transmitter at 30° w.r.t. the Z Axis

UNCLASSIFIED

SECURITY CLASSIFICATION OF THIS PAGE (When Data Entered)

REPORT DOCUMENTATION PAGE	READ INSTRUCTIONS BEFORE COMPLETING FORM
1. REPORT NUMBER: AFOSR-TR-80-0532	2. GOVT ACCESSION NO: AD-A086 884
	3. RECIPIENT'S CATALOG NUMBER
4. TITLE (and Subtitle): ANALYTICAL STUDY OF THE BISTATIC RADAR CROSS-SECTION OF A PROLATE SPHEROID	5. TYPE OF REPORT & PERIOD COVERED: FINAL 1 May 79 - 1 Feb 80
	6. PERFORMING ORG. REPORT NUMBER
7. AUTHOR(s): Albert W. Biggs, Stanton B. McMillian	8. CONTRACT OR GRANT NUMBER(s): AFOSR-79-0105
9. PERFORMING ORGANIZATION NAME AND ADDRESS: University of Kansas Center for Research, Inc. 2291 Irving Hill Drive-Campus West Lawrence, Kansas 66045	10. PROGRAM ELEMENT, PROJECT, TASK AREA & WORK UNIT NUMBERS: 61102F 2305/09
11. CONTROLLING OFFICE NAME AND ADDRESS: Air Force Office of Scientific Research/NE Bolling AFB DC 20332 Electronic & Material Sciences Directorate	12. REPORT DATE: March 1980
	13. NUMBER OF PAGES: 24
14. MONITORING AGENCY NAME & ADDRESS (if different from Controlling Office)	15. SECURITY CLASS. (of this report): Unclassified
	15a. DECLASSIFICATION/DOWNGRADING SCHEDULE

16. DISTRIBUTION STATEMENT (of this Report)

Approved for release; distribution unlimited.

17. DISTRIBUTION STATEMENT (of the abstract entered in Block 20, if different from Report)

18. SUPPLEMENTARY NOTES

19. KEY WORDS (Continue on reverse side if necessary and identify by block number)

20. ABSTRACT (Continue on reverse side if necessary and identify by block number)

Bistatic radar has important application in strategic and tactical space surveillance and in weapon tracking. At the present time, there is a lack of standard techniques for measuring radar cross sections. This effort was a feasibility study into obtaining an exact radar cross section for the Advanced Strategic Air Launched Missile (ASALM). The study was limited to the bistatic cross-section of a typical target. A prolate spheroid was selected because it resembles an air cruise missile. Results were configured in the form of bistatic-

DD FORM 1 JAN 73 1473 EDITION OF 1 NOV 65 IS OBSOLETE

UNCLASSIFIED

cross-sections with a computer program to generate additional cross-sections for prolate spheroids with different major to minor axis ratios. Any surface that is convex at each point, and which has no two distinct points where the outward normal vectors are in the same direction, can be handled similarly. Hence, the program written could very quickly be changed to handle a figure that is ellipsoidal in all the major planes, or even a parabola of revolution that extends to infinity in one direction. It is simply a matter of being able mathematically to describe the surface.